Superconducting Bi_{2}Te: Pressure-induced universality in the (Bi_{2})_{m}(Bi_{2}Te_{3})_{n} series

Ryan L. Stillwell, Zsolt Jenei, Samuel T. Weir, Yogesh K. Vohra, and Jason R. Jeffries

Phys. Rev. B **93**, 094511 — Published 9 March 2016

DOI: 10.1103/PhysRevB.93.094511

Superconducting Bi_2Te: pressure-induced universality in the $(Bi_2)_m(Bi_2Te_3)_n$ series

Ryan L. Stillwell,[1] Zsolt Jenei,[2] Samuel T. Weir, [2] Yogesh K. Vohra,[3] Jason R. Jeffries [1]

[1]*Materials Science Division, Lawrence Livermore National Laboratory, Livermore, California 94550, USA*

[2]*Physics Division, Lawrence Livermore National Laboratory, Livermore, California 94550, USA*

[3]*Department of Physics, University of Alabama at Birmingham, Birmingham, Alabama 35294, USA*

Using high-pressure magnetotransport techniques we have discovered superconductivity in Bi_2Te, a member of the infinitely adaptive $(Bi_2)_m(Bi_2Te_3)_n$ series, whose end members, Bi and Bi_2Te_3, can be tuned to display topological surface states or superconductivity. Bi_2Te has a maximum T_c= 8.6 K at P= 14.5 GPa and goes through multiple high pressure phase transitions, ultimately collapsing into a bcc structure that suggests a universal behavior across the series. High-pressure magnetoresistance and Hall measurements suggest a semi-metal to metal transition near 5.4 GPa, which accompanies the hexagonal to intermediate phase transition seen via x-ray diffraction measurements. In addition, the linearity of $H_{c2}(T)$ exceeds the Werthamer-Helfand-Hohenberg limit, even in the extreme spin-orbit scattering limit, yet is consistent with other strong spin-orbit materials. Considering these results in combination with similar reports on strong spin-orbit scattering materials seen in the literature, we suggest the need for a new theory that can address the unconventional nature of their superconducting states.

Introduction

The last several years have seen a large volume of research dedicated to materials whose properties are driven by the topology of their quantum states[1]. These states realize long theorized exotic quantum mechanical effects, such as Weyl fermions, predicted nearly a century ago, [2, 3] and others, like topological insulators (TI) and topological superconductors, only a few years ago[4, 5]. One of the more exciting prospects of TIs is that with proximity induced superconductivity[6] they provide the Z_2 non-trivial state allowing for promising applications in spintronics and quantum computation,[7] as well as the experimental realization of Majorana fermions[8].

One of the key properties necessary for making a TI is strong spin-orbit coupling, first discovered in HgTe quantum wells, and later found in several bismuth-based chalcogenides[9-12]. A particularly interesting family of these materials is the

infinitely adaptive series $(A_2)_m(A_2Q_3)_n$, with A=(Bi, Sb) and Q=(Se, Te). Though members of this series are well known as some of the best thermoelectric materials, they were recently found to be topological insulators as well[13-16]. In particular, the end members of the infinitely adaptive $(Bi_2)_m(Bi_2Te_3)_n$ series, Bi and Bi_2Te_3, can be experimentally tuned to display topological surface states or superconductivity under appropriate conditions[11, 17-19].

In our search for functional materials that possess these exotic properties we synthesized and studied Bi_2Te, a member of the $(Bi_2)_m(Bi_2Te_3)_n$ series, with m=2 and n=1. Containing a Bi fraction of 0.67, Bi_2Te is on the Bi rich side of this series, which spans the spectrum from pure Bi (m=3:n=0) to Bi_2Te_3 (m=0:n=3). Similar to other members of this series[20-22], Bi_2Te transforms from an ambient pressure semimetal to a high pressure superconductor, progressing through multiple structural and electronic phases, including a high pressure body centered cubic structure with a maximum T_c = 8.6 K at 14.5 GPa. This suggests a universal behavior seen across the $(Bi_2)_m(Bi_2Te_3)_n$ homologous series, as well as in elemental Te[23], [24], Se [25], and Bi_2Se_3 [26, 27] .

Experiment

Single crystals of Bi_2Te were grown using the self-flux method. Elemental Bi and Te (99.999%, ESPI Metals), in a ratio of 12 at.% Te and 88 at.% Bi, were combined in an alumina crucible and sealed under 500 mbar of high purity argon gas in a quartz tube and melted at 420 ^oC for 2 days. The solution was then cooled to 318 ^oC over a period of 4 days, at which point the quartz tube was removed from the oven and centrifuged to remove excess flux. Large platelets were removed and ground into a coarse powder using a mortar and pestle. The coarse powder was then placed on a glass slide and chopped with a razor blade into a fine powder for powder x-ray diffraction characterization. These measurements confirmed that the lattice parameter is consistent with literature and that they were single phase Bi_2Te[13]. Additionally, we did not observe any peak-broadening effects that might be expected if there were any core-shell crystals indicating compositional gradients.

For structural studies under pressure we used a conventional, membrane-driven diamond anvil cell (DAC) with 300μm diamond culets. The powdered Bi_2Te, 3-5μm particle size, was loaded into a 130-μm diameter sample chamber that was drilled out of a rhenium gasket preindented to 25 GPa, corresponding to an initial thickness of 23 μm. The chamber was also loaded with, fine copper powder (3-6μm, Alfa Aesar) as the pressure calibrant and neon, precompressed to 30,000 psi, as the pressure-transmitting medium. Room-temperature, angle-dispersive x-ray diffraction experiments were performed at HPCAT (beamline 16 BM-D) at the Advanced Photon Source at Argonne National Laboratory. The sample was illuminated with a 29.2 keV monochromatic x-ray beam and angular dispersive diffraction patterns were collected with a Perkin Elmer detector using an exposure time of 10-20 s. The two dimensional diffraction images were integrated using Fit2D,[28] then analyzed using the JADE software package to extract crystal structure and volume information. To determine the pressure, we used the Vinet equation of state of the copper, with fitting parameters for the bulk modulus B_0=133 GPa and its pressure derivative B_0'=5.01 from Dewaele et al.[29]

For electrical transport studies under pressure we used an eight-probe designer DAC[30, 31] with 280μm diameter culets, steatite as a pressure-transmitting medium and ruby as the pressure calibrant. [32, 33] A MP35N metal gasket was preindented to an initial thickness of 60 μm, and a 120 μm hole was drilled in the center of the indentation for the sample chamber using an electric discharge machine. A small crystal of Bi_2Te with dimensions of 80-μm diameter and 10-μm thick, was taken out of the larger, micaceous crystallites and placed onto the designer anvil to ensure electrical contact with the tungsten leads exposed on the face of the designer diamond culet. Pressure was measured at room temperature on two separate ruby spheres within the sample chamber in order to estimate pressure distribution across the chamber. Based on previous studies using this type of DAC the error in the pressure at low temperatures was estimated to be 5%[31]. Temperature was measured using a calibrated Cernox thermometer affixed to the outside of the DAC. Electrical transport measurements were made as a function of

temperature and magnetic field using the AC Transport option in the Quantum Design PPMS.

Results

High pressure x ray diffraction studies were performed on Bi_2Te powder in order to explore the universality of the collapse into the high pressure body-centered-cubic (bcc) phase that occurs within the $(Bi_2)_m(Bi_2Te_3)_n$ series. At ambient pressure and temperature the Bi_2Te starts out in the hexagonal phase with the *P-3m* crystal structure, denoted as Bi_2Te-I, which persists up to 7 GPa. Upon compression near 5 GPa an intermediate phase begins to appear, denoted as Bi_2Te-II. Diffraction peaks belonging to this Bi_2Te-II phase are present in the diffraction patterns up to 17 GPa. However, at 9 GPa a second phase transition begins into the Bi_2Te-III that completes at 17 GPa. Integrated diffraction patterns for the three phases are shown in figure 1. Bi_2Te-II has a very broad pressure range where it coexists with either phase I or phase III, but only a small 2 GPa window in which it is the only phase observed. Within this small window, we were unable to index the peaks to a structure with a pressure-volume dependence that was consistent with phases I and III In contrast, the high pressure Bi_2Te-III can easily be indexed to the bcc (*Im-3m*) unit cell with a=3.747 Å at P= 8.8 GPa and it is the stable phase to 47 GPa, the highest pressure attained in this study. Fitting the pressure-volume data points to the Vinet EOS[34, 35] for phase III we obtain V_o= 29.88 ($\pm$0.27)Å, B_o=54.2 ($\pm$5) GPa and $B' = 4.78(\pm 0.32)$. This Bi_2Te-III structure is best understood as a disordered substitutional alloy, such that the bismuth and tellurium atoms reside randomly on the (2a) site of the bcc structure with occupancies defined by the 2:1 Bi:Te stoichiometry of the sample. This is believed to be due to the similar atomic radii of the two elements and is further enabled by charge transfer as a result of the application of high pressure. This behavior has also been seen in similar materials such as $(Bi,Sb)_2Te_3$ and Bi_4Te_3. [20, 36-38] Furthermore it seems that the unit cell volume as a function of pressure for the *bcc*-phase in Bi_2Te follows the same P-V curve as do the above mentioned two compounds (fig. 2(a)). We also note that concomitant with the phase transformation from phase I to phase III, there is a

volume collapse of approximately 9%. The fact that Bi_2Te also collapses into the bcc phase *strongly* suggests that, despite having disparate ground state phases, the entire $(Bi_2)_m(Bi_2Te_3)_n$ series converges into the bcc phase at high pressures. These structural transformations are ubiquitous across this series, which suggests that there should also be concurrent transformations occurring in the electronic structure as well.

High-pressure magnetotransport measurements were performed to investigate the effects of the high-pressure structural phase transformations on the electronic structure of Bi_2Te. Hall resistance at 25K as a function of applied magnetic field is shown in Figure 3 for selected pressures. It can be seen that there is a clear change in the Hall resistance between 5.4 and 7.6 GPa, coincident with the phase transformation from the hexagonal phase (Bi_2Te-I) to the intermediate, mixed phase (Bi_2Te-II) observed in x-ray diffraction. Although the structural and electronic phase transitions occur at nearly the same pressure, the difference in the two transitions pressures could be attributed to the different pressure media used in the two experiments. The neon gas used in the diffraction measurements is considered hydrostatic up to about 10 GPa [39], whereas the steatite used in the magnetotransport measurements is a solid medium that can support small pressure gradients. Nonetheless, the fact that both phase diagrams agree as well as they do shows that pressure medium is not affecting the structure or phase transformation mechanisms, though it is worth considering that it may be affecting some subtle electronic properties that are below the resolution of this study. The linearity of R_{xy} as a function of applied magnetic field suggests a dominant carrier type (fig. 3) for all pressures at T=25K, but for pressures below 9.2 GPa a multiband picture of Bi_2Te emerges in the temperature dependence of the Hall coefficient (fig. 4). At 2.8 GPa there is a crossover from negative to positive Hall coefficient near 70K demonstrating a change in the dominant charge carrier type. From our x-ray diffraction measurements we know that Bi_2Te is in a mixed phase regime above 5 GPa, but as pressure is increased above 2.8 GPa the crossover temperature in the Hall sign decreases, as does the magnitude of the Hall coefficient, suggesting a net

increase in the carrier density as a function of pressure. In the mixed phase above 5.4 GPa there is very little change in the carrier concentration, compared to the concentration in the low-pressure, hexagonal phase, Bi_2Te-I. This can be clearly seen in figure 2(b), where the slope of the Hall resistance versus applied field, R_H, and the longitudinal resistance, R_{xx}, are plotted as a function of pressure. The Hall coefficient, R_H, as defined above as the slope of the Hall resistance as a function of applied magnetic field, is inversely proportional to the carrier density and, if the carrier concentrations are calculated using a single band model, there is an increase in carrier concentration within order of magnitude from $\sim 10^{21}$ cm^{-3} at 2.8 GPa—more typical of a semimetal— to $\sim 10^{23}$ cm^{-3} for pressures of 6.4 GPa and above—more characteristic of a typical metal. Considered within the single band model, this suggests that there is a metallization of Bi_2Te at these higher pressures there should now be more electrons available to form superconducting pairs, as has been seen in many of the other members of the $(Bi_2)_m(Bi_2Te_3)_n$ series[17, 18, 20].

Low-temperature, high-pressure transport data (Fig. 5) shows the onset of superconductivity at 11.5 GPa. Though Bi_2Te did not fully enter the superconducting state by our minimum temperature of 1.8K, we can extrapolate that the midpoint of the transition should have a T_c ≈ 2.1 K (see fig. 5). At the next pressure, P = 12.9 GPa, there are two transitions visible as it enters the superconducting state. This correlates with the fact that the system is in the intermediate Bi_2Te-II and Bi_2Te-III mixed phase, with a different T_c for the two states (see fig. 2(c)). T_c increases sharply between 11.5-12.9 GPa for both transitions, with $T_{c,II}$= 5.8K and $T_{c,III}$= 7.7K. Once the pressure is increased to P= 14.5 GPa there is a single, sharp superconducting transition, which gives the maximum T_c= 8.6 K with a transition width of only 0.57 K. Although from the x-ray diffraction data we know that Bi_2Te is still in the mixed phase at P= 14.5 GPa, the superconducting transition seems dominated by the Bi_2Te-III (bcc) phase, and has a T_c similar to the maximum T_c of Bi[17], Bi_4Te_3[20] (both 8.4 K), and Bi_2Te_3 [18](9.3 K) under pressure, all of which transform into a high-pressure bcc phase. After reaching its maximum, T_c decreases monotonically down to T_c = 4.9 K at 32 GPa.

The universality of the superconducting state of the $(Bi_2)_m(Bi_2Te_3)_n$ series in the high-pressure bcc phase can be seen more clearly by plotting the reduced critical temperature, $T_c/T_{c,max}$ versus $P/P_{c,max}$, where $P_{c,max}$ is the pressure where $T=T_{c,max}$, as is shown in figure 2(c) inset. This shows the linear trend common to the series as T_c is suppressed by increasing pressure after reaching $T_{c,\,max}$ at a rate dT_c/dP= -0.34±0.02 K/GPa. The linear suppression of T_c is consistent with BCS-type phonon-mediated superconductivity in Bi_2Te, in which pressure raises the average phonon frequency and reduces the electron-phonon coupling, thus decreasing the pairing mechanism strength. [40, 41] To further investigate the nature of the superconducting state using a treatment consistent with a BCS superconducting state, we can look at the electron-phonon coupling through the McMillan formula to find the volume Grüneisen parameter and compare it with other BCS superconductors.

The McMillan formula is given as T_c= (<ω>/1.2)exp([-1.04(1+λ)]/[λ-μ*(1+0.62λ)]), valid in the strong coupling regime (λ≤1.5), and connects T_c with the electron-phonon coupling parameter λ, an average phonon frequency <ω>, and the screened Coulomb repulsion μ* (taken here to be 0.1).[42] By taking the logarithmic volume derivative of T_c, we get the relation

$$\frac{d\ln T_c}{d\ln V} = -\gamma + \Delta\left\{\frac{d\ln \eta}{d\ln V} + 2\gamma\right\},$$

in which γ= $-d\ln\langle\omega\rangle/d\ln V$ is the Grüneisen parameter, η= $N(E_f)\langle I^2\rangle$ is the Hopfield parameter, which is given by the product of the electronic density of states and the average-squared electronic matrix element, and Δ= $1.04\lambda[1+0.38\mu^*]/[\lambda-\mu^*(1+0.62\lambda)]^2$. [43] Although the average phonon frequency <ω> has not been determined experimentally for Bi_2Te at high pressure, we can test a range of values of 100, 200, and 300K, that cover the range of the typical values. We choose P= 14.5 GPa, where T_c is a maximum at 8.6 K, to look at these values. Substituting T_c= 8.6 K, <ω> =100K, and μ* =0.1 into the McMillan equation and solving for λ, we find λ=1.17. We can then substitute this value into the equation for Δ, which gives a value

of Δ=1.28. All of these values can then be substituted into the above equation to find γ. We can extract the value of $d \ln T_c / d \ln V$ from our experimental data by combining our equation of state data (Fig. 4a) with the superconducting phase diagram (Fig. 4c). If we plot ln T_c vs ln V and take the derivative near P= 14.5 GPa, we find a value of $d \ln T_c / d \ln V$ =5.55 K/Å^3. Substituting this value into the above equation for γ, along with our value of Δ, and taking the value of $d \ln \eta / d \ln V$= -1,[44] assuming again that Bi_2Te behaves like a simple p-electron metal, we are able to extract a value of γ= 4.38. To test the parameters of this calculation we can vary the value of <ω>= 200 and 300K, which gives values of γ= 2.3 and 1.9, respectively, closer to that of tin (γ≈+2.1).[45] While yielding a γ value closer to that expected for simple metals like Sn, <ω>=200 or 300 K are substantially higher values than that of Sn (<ω> ≈ 110K).[42] Given the strong compression of the lattice at the pressures where superconductivity is observed, it is likely that there is commensurate phonon stiffening, which would serve to increase <ω>. In light of this potential phonon stiffening, a value of <ω>=200 K does not seem unreasonable, and therefore the associated γ may be a reasonable estimate. Even with uncertainties in <ω>, the γ values calculated for Bi_2Te suggest that it behaves like a simple, BCS type phonon-mediated superconductor in the high-pressure, bcc phase. Future experiments studying the high-pressure phonon dispersions in Bi_2Te are needed to determine the actual value of <ω> and thereby more accurately determine the nature of the superconducting state in Bi_2Te, and possibly the rest of the homologous series.

To investigate the pair-breaking mechanism in greater detail we applied magnetic fields to study how the superconducting state is suppressed as a function of pressure and magnetic field. This is shown for a single pressure of P= 14.5 GPa for applied fields up to 30 kOe (Fig. 6), but was performed at all of the pressures in order to understand the pressure evolution of the superconducting state. Figure 7 shows the rate of suppression of T_c with applied magnetic field at all pressures up to 32.0 GPa. T_c is defined as the midpoint of the superconducting transition, and only needed to be estimated for the highest applied magnetic fields, except at P=28.7 GPa. The estimated superconducting transition temperatures for the extrapolated data

were based on a linear extrapolation of the resistance versus temperature curve for temperatures where $T_{midpoint}<T_{final}<T_{onset}$. The rate of suppression is quasilinear at all pressures down to the lowest temperatures measured. This quasilinear trend of $H_{c2}(T)$ has also been observed in Bi_4Te_3 [20], Bi_2Se_3 [26], $Cu_xBi_2Te_3$ [46], as well as YPtBi [47, 48] and ErPdBi [49]. Considering that all of these materials contain bismuth, these results suggest that strong spin-orbit scattering is the dominant pair breaking mechanism in these materials.

As a starting point to analyze superconductivity in Bi_2Te we begin by assuming that it is a conventional superconductor. This is supported by the linear suppression of T_c as a function of pressure in Bi_2Te [42]. In fact, the canonical model for this analysis, developed by Werthamer, Helfand and Hohenberg (WHH) [50], was originally applied to a Ti-Nb alloy with a bcc structure, similar to that of Bi_2Te, and contains a parameter which incorporates spin-orbit effects, which are germane to any modeling of Bi containing systems. Within the WHH model for orbitally limited superconductors we can calculate the upper critical field at P= 14.5 GPa as $H_{c2}(0)= -0.7\ T_c \times dH_{c2}/dT|_{T=Tc}= 1.94$ T, where $T_c(H=0) = 8.66$ K taken at the midpoint of the superconducting transition, and $dH_{c2}/dT =-0.321$ T/K . This is lower than the measured $H_{c2}(2K)= 2.12$ T, suggesting that there is another mechanism involved in the superconducting pair breaking. If H_{c2} is Pauli limited, then the superconducting gap energy Δ is equal to the Zeeman energy and therefore the Pauli limiting field $H_P=1.84T_c= 15.93$ T at P= 14.5 GPa. Since the measured H_{c2} is higher than the orbital limit but significantly lower than H_P, we can assume that both orbital and Pauli limiting effects are in play, with the orbital mechanism being the dominant one. To incorporate both mechanisms into our calculations of H_{c2}, we can recalculate H_{c2} using the modified formula, which includes the Maki parameter $\alpha= \sqrt{2}\ H_{c2}^{orb}/\ H_p$ [51], so that $H_{c2}^{\alpha}= H_{c2}^{orb}/\sqrt{(1+\alpha^2)}=1.79$ T at P=14.5 GPa, where α=0.172, $H_{c2}^{orb}= 1.94$ T, and $H_P= 15.93$ T. Including the Maki parameter only lowers the calculated $H_{c2}(T)$, providing further evidence that the pair breaking in Bi_2Te is driven by spin-orbit scattering and not Pauli spin-paramagnetism.

To compare our results within the WHH theory for spin-singlet superconductors we plot the normalized critical field $h^*(t)=(H_{c2}/T_c)/|dH_{c2}/dT|_{t=1}$ as a function of the normalized temperature $t=T/T_c$ for selected pressures up to 32 GPa (figure 8). The error bars in figure 8 are determined by propagating the individual uncertainties (e.g., ΔTc) in the parameters defining h^* and t. Since we define T_c as the midpoint of the superconducting transition, the error in T_c is defined as the accuracy of the measurement of the resistance at T_c, where $\Delta R/R$ is ±1%. Given that the temperature is accurate to ±1%, we take whichever is the larger of the two as the error in T_c. Due to trapped magnetic flux within the magnet, there is an uncertainty in the applied field of 0.1 kOe: $\Delta Hc2$=0.1 kOe. The error in $|dH_{c2}/dT|_{t=1}$ is defined from the standard deviation returned from linear fits to the data near t=1. Because the critical field curves exhibit strong linearity, the slope near t=1 can be determined with an error below 2%.

All of the pressures follow the same $h^*(t)$ slope and remain linear down to the lowest temperatures measured of t~0.3. Based on the strong spin-orbit effects of Bi based materials, we assumed that spin-orbit scattering was the main contributor to the pair-breaking mechanisms in Bi_2Te and therefore we include spin-orbit effects (λ_{so}) within the WHH formalism, in a similar fashion to reference [52], and compare them to our experimental results (Fig. 8): the blue, dashed line is the WHH in the dirty limit (α=0); the red, dashed line includes a value of α=0.2 (close to our experimental value of 0.172 calculated for P= 14.5 GPa) and λ_{so}=0; and the black, dashed line includes α=0.2 and an unphysically large λ_{so}=100. The addition of α=0.2 shifts the $h^*(t)$ curve down only slightly, and only for t≤0.3. Because α is so small in Bi_2Te, increasing λ_{so} barely shifts the $h^*(t)$ curve up even for λ_{so}=100, a spin-orbit scattering strength, which is well outside the limits of WHH. Considering that our data deviate from all of these models below t~0.5, it is clear that a theory which includes very strong spin-orbit interactions must be developed to deal with this and similar spin-orbit driven superconductors, as attested to by a growing body of experimental work[26, 46, 48, 53].

In conclusion, we have found that Bi_2Te provides further evidence of a universal behavior of the series to collapse into the bcc structure at high-pressure. Although Bi_2Te enters a high-pressure mixed phase region between roughly 5-17 GPa, we were able to observe a semimetal-metal transition near 5.4 GPa in both linear and Hall resistance measurements. We were able to establish that there is a dominant carrier type below 5.4 GPa via magnetic field and temperature dependence measurements, though it was difficult to unambiguously determine carrier type and concentration in the mixed phase. We also made the first discovery of pressure induced superconductivity in Bi_2Te, with a maximum T_c=8.66K at P= 14.5 GPa. Bi_2Te has a similar maximum T_c (~8K) to other materials in the $(Bi_2)_m(Bi_2Te_3)_n$ series, as well as a similar rate of suppression of T_c with pressure. Analysis of the pressure-dependence of the superconducting state suggests that Bi_2Te is likely a conventional, BCS superconductor, but the linear suppression of T_c with field implies unconventional and strong spin-orbit scattering pair-breaking effects. This pair-breaking is outside of the scope of the conventional WHH theory and requires a new treatment that is able to incorporate strong spin-orbit scattering. Although establishing whether Bi_2Te has topologically nontrivial surface states is outside the scope of this paper, as a member of the homologous series $(A_2)_n(A_2B_3)_m$, where A=Bi, Sb, Pb, Ge and B=Te, Se, S, many permutations and dopings of these and similar materials[14, 15, 46, 54-56] have produced TIs. It would be of great interest if future work could confirm whether Bi_2Te is a TI via theoretical calculations as well as experimental techniques like ARPES, STM or quantum oscillations. This would help to confirm the universality of the infinitely adaptive $(Bi_2)_m(Bi_2Te_3)_n$ series, not only with regard to the superconducting state and high-pressure crystal structure, but also in the topological nature of these materials as well.

This work was performed under LDRD (Tracking Code 14-ERD-041) and under the auspices of the US Department of Energy by Lawrence Livermore National Laboratory (LLNL) under Contract No. DE-AC52- 07NA27344. Portions of this work were performed at HPCAT (Sector 16), Advanced Photon Source (APS), Argonne National Laboratory. HPCAT operations are supported by DOE-NNSA under Award

No. DE-NA0001974 and DOE-BES under Award No. DE-FG02-99ER45775, with partial instrumentation funding by NSF. The Advanced Photon Source is a U.S. Department of Energy (DOE) Office of Science User Facility operated for the DOE Office of Science by Argonne National Laboratory under Contract No. DE-AC02-06CH11357. Beamtime was provided by the Carnegie DOE-Alliance Center (CDAC). YKV acknowledges support from DOE-NNSA Grant No. DE-NA0002014.

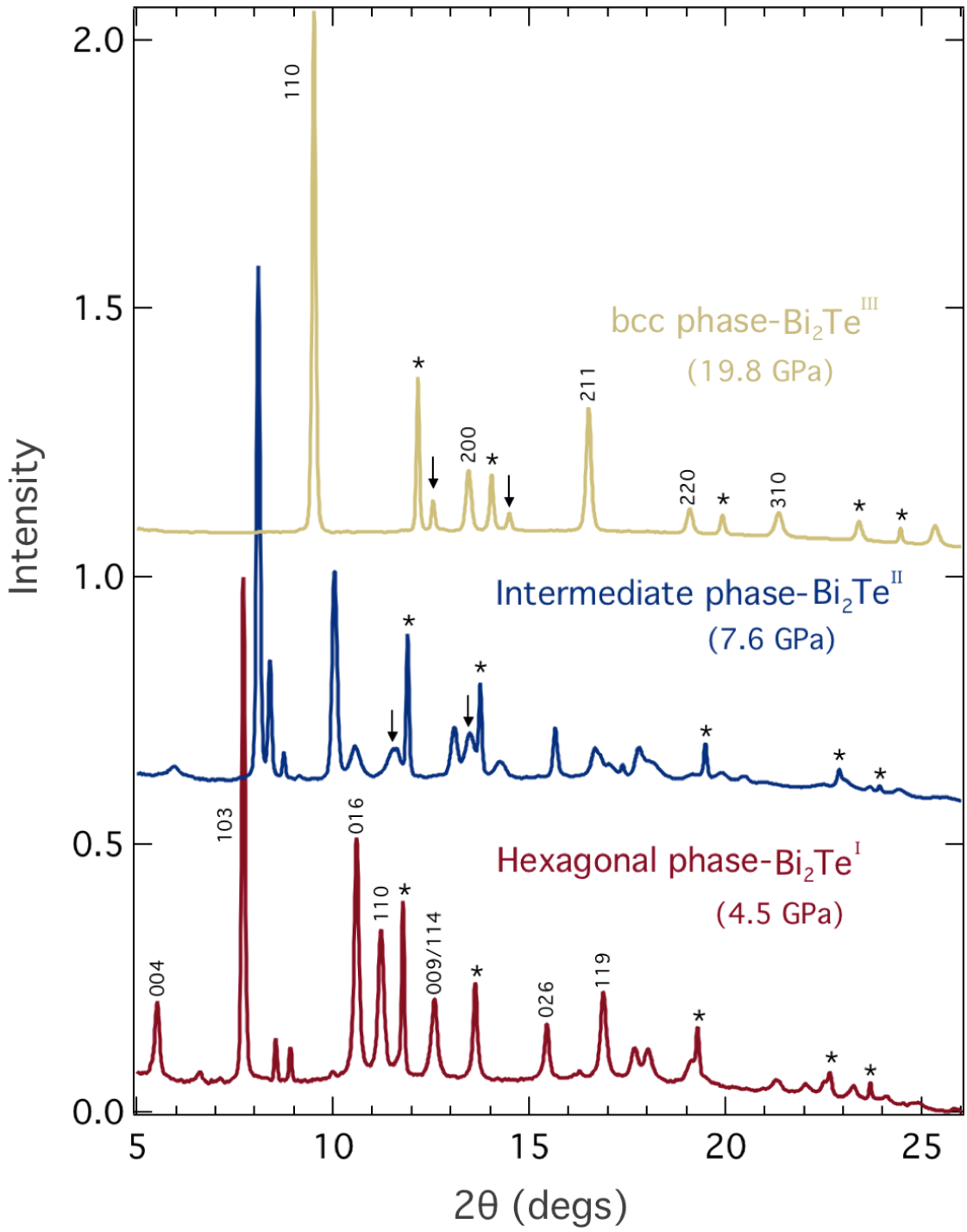

FIG. 1 (Color online) **X-ray diffraction patterns at pressures within the hexagonal (P<5 GPa), intermediate (5 GPa <P<17 GPa) and body-centered-cubic phases (P>17 GPa). The *h k l* indices of some of the diffraction reflections are shown for the hexagonal and bcc phase of Bi_2Te. Stars are the peaks from the copper pressure calibrant and the arrows show the peaks due to the neon pressure medium.**

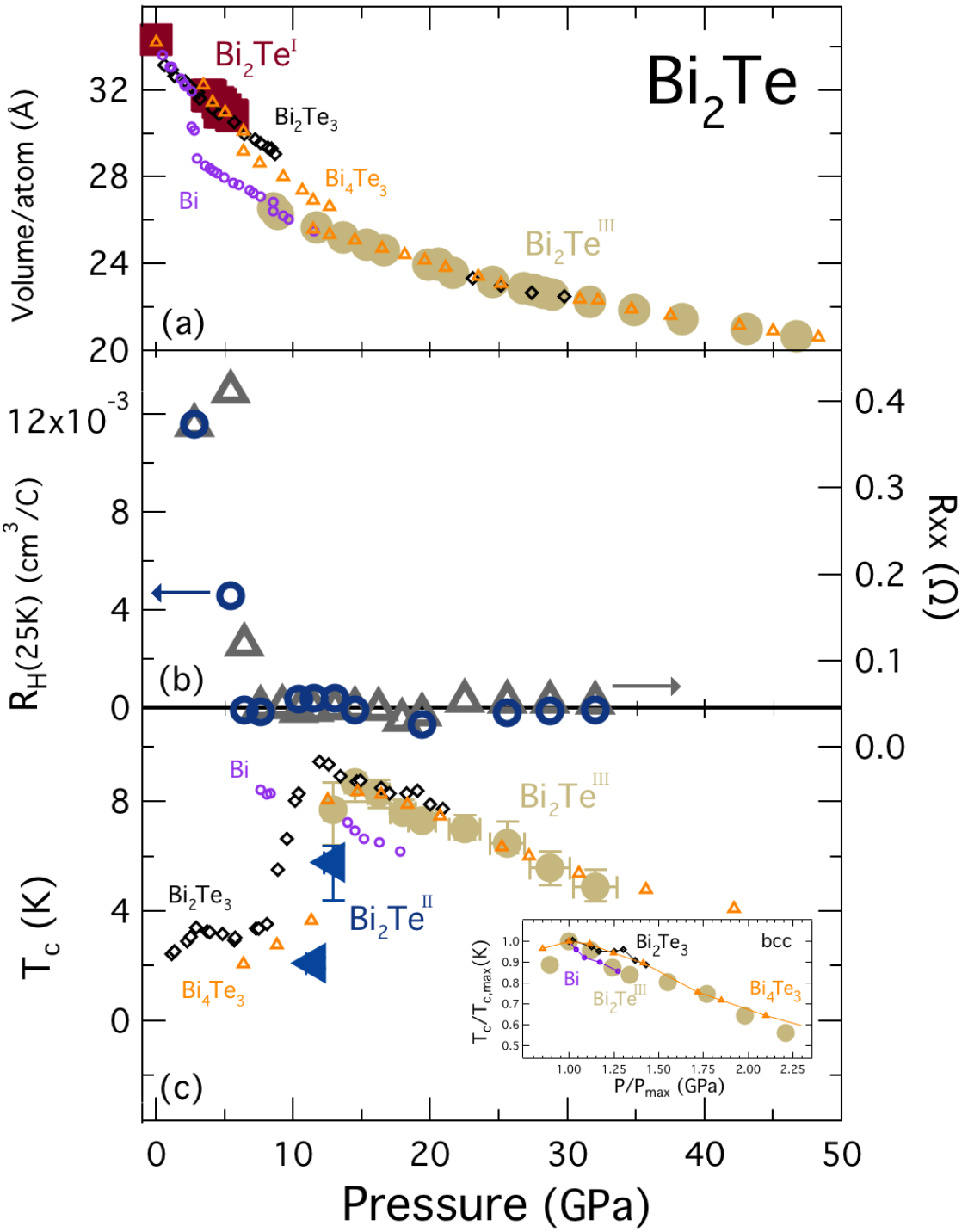

FIG.2 (Color online) (a) Bi_2Te shows universal behavior in the high pressure phase as it collapses into the bcc phase, just as the other members of the infinitely adaptive $(Bi_2)_m(Bi_2Te_3)_n$ series do. This result confirms this family of compounds, with disparate electronic and crystal structure ground states, can be tuned by the application of pressure to elicit a universal metallic, superconducting phase with the body-centered cubic crystal structure. (b) The electronic phase transitions that accompany the structural transitions are seen in the semimetal to metal crossover near 5 GPa, as well as the change in charge

carrier type between 10-14 GPa. R_H is given as the slope of the Hall resistance, R_{xy}, versus the applied magnetic field (fig. 3) (c) T_c as a function of pressure for Bi_2Te plotted with the other members of the homologous family showing similar trends for peaks of T_c before entering the bcc phase. (c, inset) T_c normalized to maximum T_c in the bcc phase to show the same relation of slope for T_c vs pressure in the bcc phase for the entire $(Bi_2)_m(Bi_2Te_3)_n$ series.

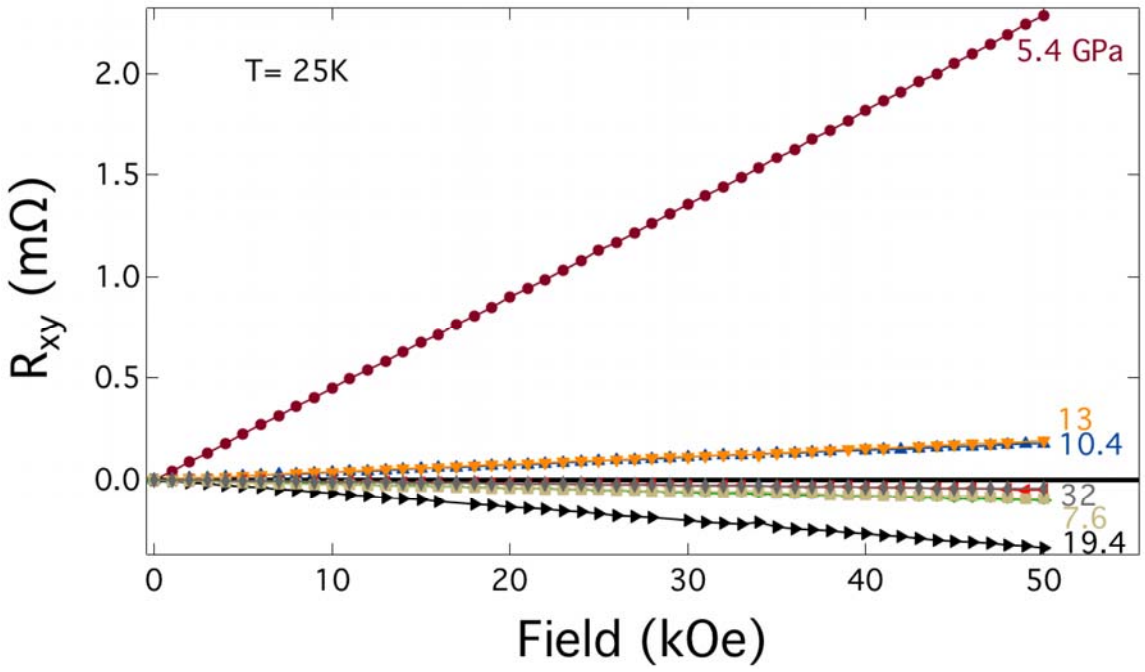

FIG. 3 (Color online) Hall resistance at 25 K as a function of applied magnetic field for pressures between 5.4-32 GPa. There is a significant decrease in the Hall resistance above 5.4 GPa, which indicates a drastic change in the carrier concentration. Also, the change in the sign of the slope indicates that the majority carrier changes as pressure is increased, though the fact R_{xy} vs H remains linear up to 50 kOe suggests that there is a single dominant charge carrier for all of the pressures studied.

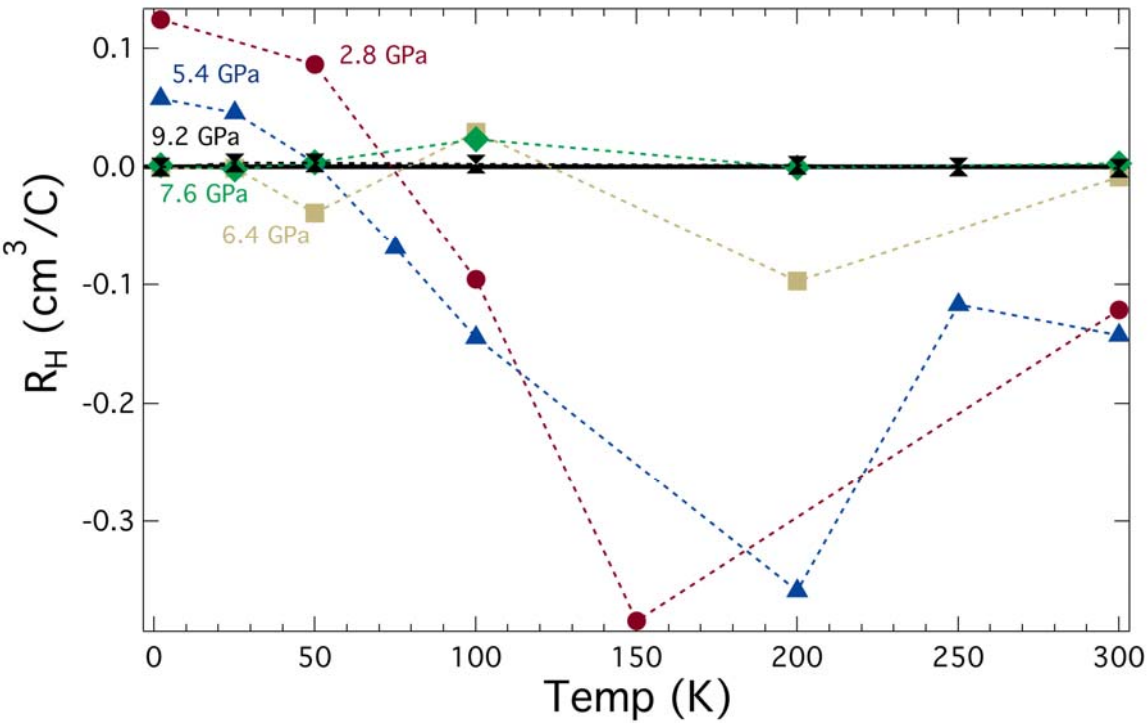

FIG.4 (Color online) Hall coefficient (linear fit to the data shown in fig.3) plotted as a function of temperature at increasing pressures shows the suppression of the carrier crossover from near 70K at 2.8 GPa to 50K at 5.4 GPa until it is nearly flat by 7.6 GPa, with no visible change in carrier as a function of temperature. Though it is difficult to interpret these results given that the system is in the intermediate, mixed phase region above 5 GPa, this figure shows that both temperature and pressure (fig. 2b) affect the band structure of Bi_2Te and drive it from a semimetal to a metal via two separate tuning parameters.

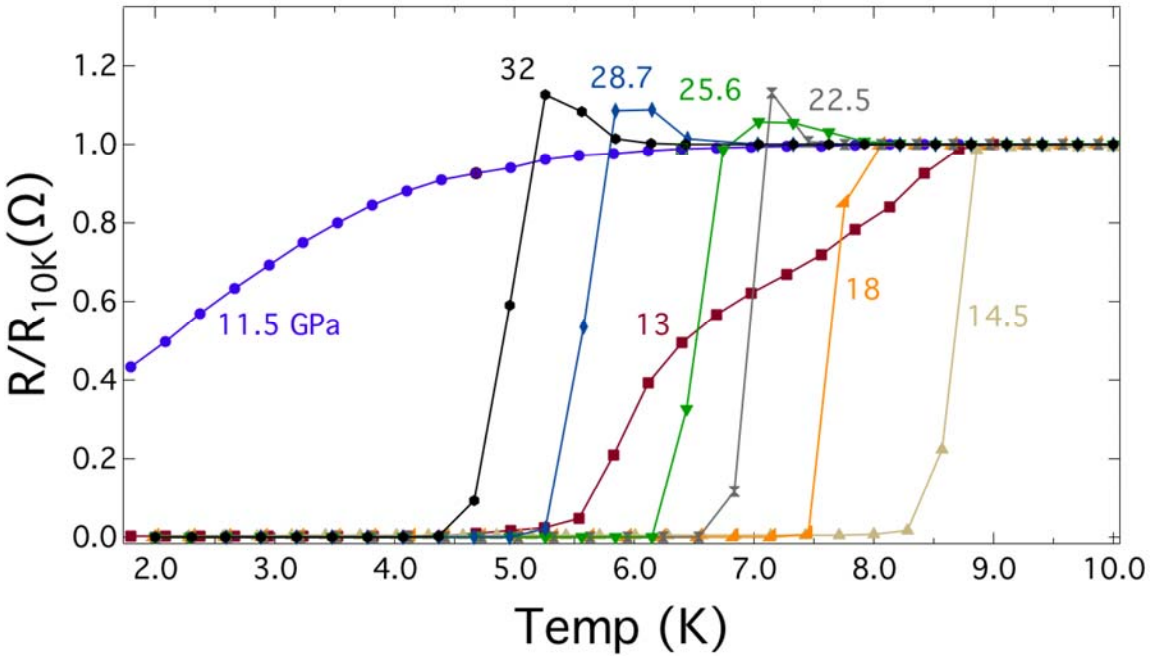

FIG.5 (Color online) Resistance as a function of temperature for pressures from 11.5-32 GPa showing the onset and subsequent suppression of the superconducting state in Bi_2Te. The resistance is normalized to the value of the resistance at 10K for each particular pressure just to emphasize the change in T_c as a function of pressure.

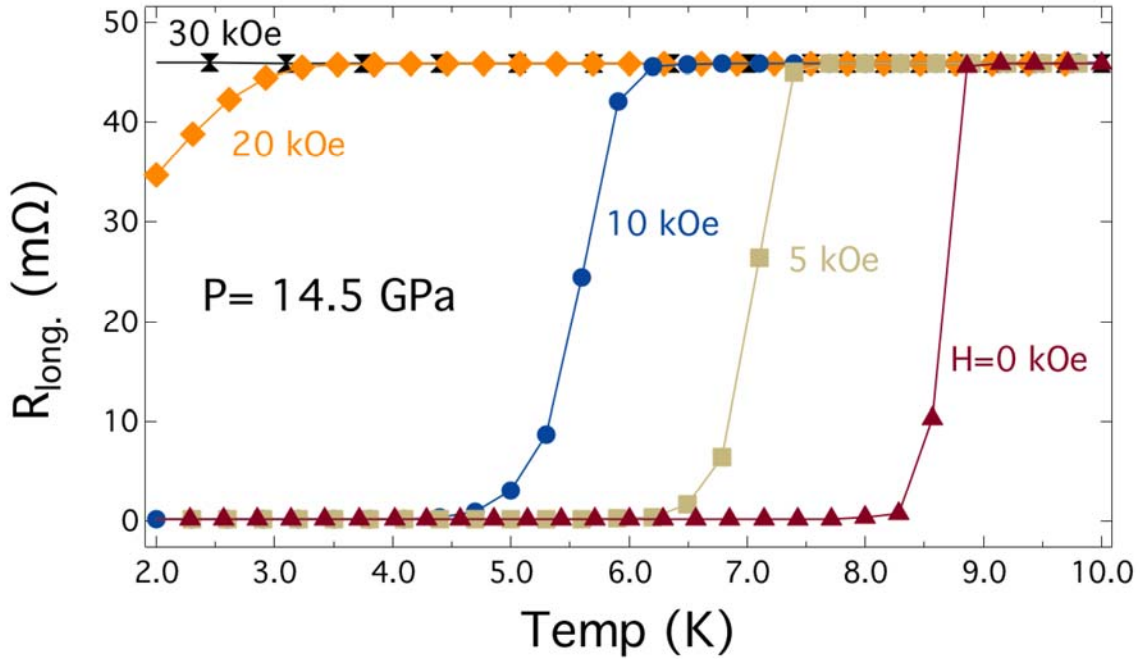

FIG. 6 (Color online) Suppression of the superconducting transition with magnetic field at P=14.5 GPa shown in plots of resistance as a function of temperature. The linear trend of dT_c/dH can be more clearly seen in the phase diagram shown in figure 7.

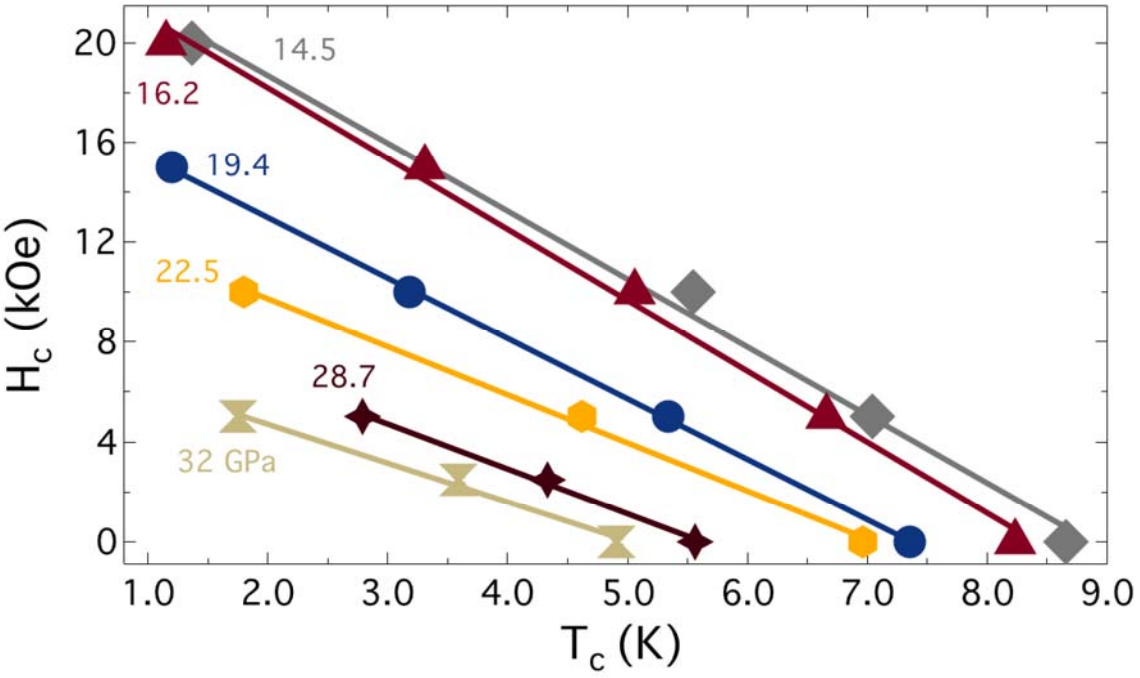

FIG. 7 (Color online) H_c is suppressed linearly with temperature for all of the pressures studied. T_c is taken to be the midpoint of the superconducting transition. Error bars are smaller than the marker size (see text).

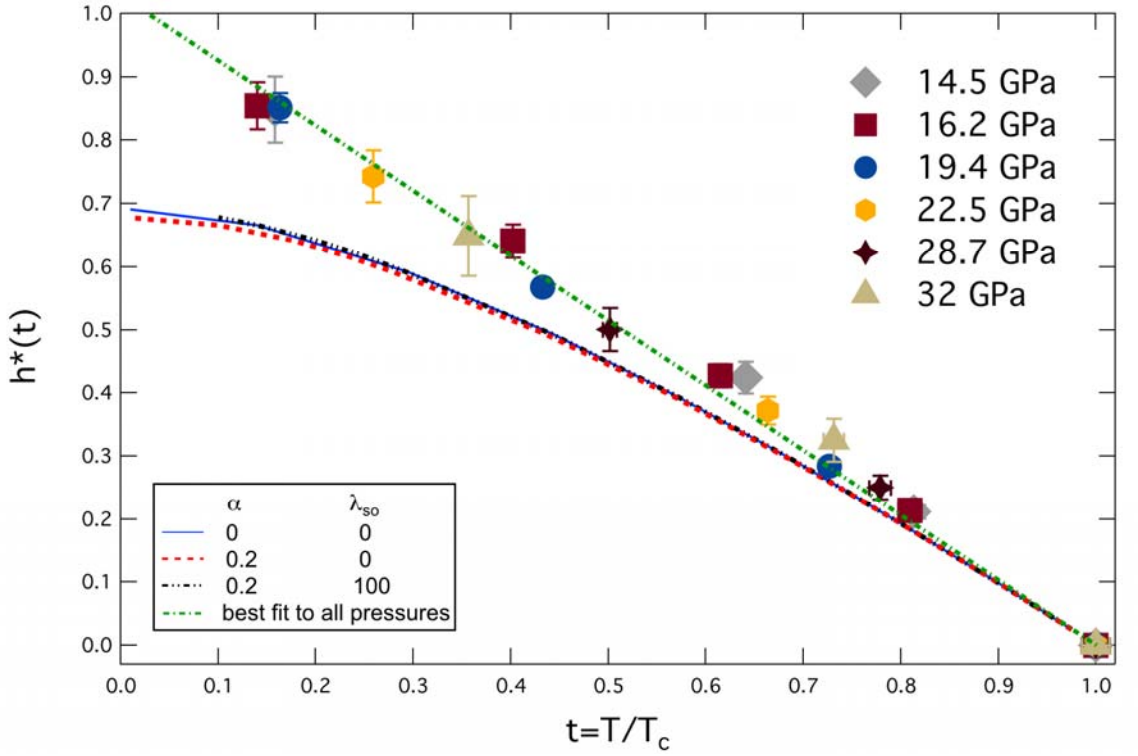

FIG. 8 (Color online) Graph showing the renormalized $H_{c2}(T)$ for selected pressures using the reduced temperature T/T_c, and the reduced critical field (see text) in order to compare with theory. The fitting is done using the classical WHH model in which the blue dashed line is the limit of the Maki parameter, $\alpha=0$ and the spin-orbit scattering strength, $\lambda_{so}=0$. To compare our data with the WHH model we used $\alpha=0.2$ and varied λ_{so} to see the effect of spin-orbit scattering. As is shown in the figure, due to the fact that α is so small, even with values of λ_{so} up to 100 (well outside of WHH conditions) our data begins to deviate from the models for $t<0.7$. Error bars are propagated from uncertainties in the measured quantities (see text).

[1] M.Z. Hasan, C.L. Kane, Colloquium: Topological insulators, Reviews of Modern Physics, 82 (2010) 3045-3067.
[2] S.-Y. Xu, I. Belopolski, N. Alidoust, M. Neupane, G. Bian, C. Zhang, R. Sankar, G. Chang, Z. Yuan, C.-C. Lee, S.-M. Huang, H. Zheng, J. Ma, D.S. Sanchez, B. Wang, A. Bansil, F. Chou, P.P. Shibayev, H. Lin, S. Jia, M.Z. Hasan, Discovery of a Weyl fermion semimetal and topological Fermi arcs, Science, 349 (2015) 613-617.
[3] H. Weyl, Elektron und Gravitation. I, Z. Physik, 56 (1929) 330-352.
[4] C.L. Kane, E.J. Mele, Z2 topological order and the quantum spin Hall effect, Physical Review Letters, 95 (2005) 146802.
[5] J.E. Moore, L. Balents, Topological invariants of time-reversal-invariant band structures, Physical Review B, 75 (2007) 121306.
[6] L. Fu, C.L. Kane, Superconducting proximity effect and Majorana fermions at the surface of a topological insulator, Physical Review Letters, 100 (2008) 096407.
[7] A.Y. Kitaev, Fault-tolerant quantum computation by anyons, Annals of Physics, 303 (2003) 2-30.

[8] F. Wilczek, Majorana returns, Nature Physics, 5 (2009) 614-618.
[9] B.A. Bernevig, T.L. Hughes, S.-C. Zhang, Quantum Spin Hall Effect and Topological Phase Transition in HgTe Quantum Wells, Science, 314 (2006) 1757-1761.
[10] M. König, S. Wiedmann, C. Brüne, A. Roth, H. Buhmann, L.W. Molenkamp, X.-L. Qi, S.-C. Zhang, Quantum Spin Hall Insulator State in HgTe Quantum Wells, Science, 318 (2007) 766-770.
[11] D. Hsieh, Y. Xia, L. Wray, D. Qian, A. Pal, J.H. Dil, J. Osterwalder, F. Meier, G. Bihlmayer, C.L. Kane, Y.S. Hor, R.J. Cava, M.Z. Hasan, Observation of Unconventional Quantum Spin Textures in Topological Insulators, Science, 323 (2009) 919-922.
[12] Y. Xia, D. Qian, D. Hsieh, L. Wray, A. Pal, H. Lin, A. Bansil, D. Grauer, Y.S. Hor, R.J. Cava, M.Z. Hasan, Observation of a large-gap topological-insulator class with a single Dirac cone on the surface, Nature Physics, 5 (2009) 398-402.
[13] J.W.G. Bos, H.W. Zandbergen, M.H. Lee, N.P. Ong, R.J. Cava, Structures and thermoelectric properties of the infinitely adaptive series (Bi2)m(Bi2Te3)n, Physical Review B, 75 (2007) 195203.
[14] R.J. Cava, H. Ji, M.K. Fuccillo, Q.D. Gibson, Y.S. Hor, Crystal structure and chemistry of topological insulators, Journal of Materials Chemistry C, 1 (2013) 3176-3189.
[15] Y. Ando, Topological Insulator Materials, Journal of the Physical Society of Japan, 82 (2013) 102001.
[16] S. Scherrer, H. Scherrer, Bismuth Telluride, Antimony Telluride, and Their Solid Solutions, in: CRC Handbook of Thermoelectrics, CRC Press, 1995.
[17] M.A. Ilina, E.S. Itskevich, Superconductivity of Bismuth Telluride, Fizika Tverdogo Tela, 13 (1971) 2496-2499.
[18] C. Zhang, L. Sun, Z. Chen, X. Zhou, Q. Wu, W. Yi, J. Guo, X. Dong, Z. Zhao, Phase diagram of a pressure-induced superconducting state and its relation to the Hall coefficient of Bi2Te3 single crystals, Physical Review B, 83 (2011) 140504.
[19] Y.L. Chen, J.G. Analytis, J.-H. Chu, Z.K. Liu, S.-K. Mo, X.L. Qi, H.J. Zhang, D.H. Lu, X. Dai, Z. Fang, S.C. Zhang, I.R. Fisher, Z. Hussain, Z.-X. Shen, Experimental Realization of a Three-Dimensional Topological Insulator, Bi2Te3, Science, 325 (2009) 178-181.
[20] J.R. Jeffries, A.L. Lima Sharma, P.A. Sharma, C.D. Spataru, S.K. McCall, J.D. Sugar, S.T. Weir, Y.K. Vohra, Distinct superconducting states in the pressure-induced metallic structures of the nominal semimetal Bi4Te3, Physical Review B, 84 (2011) 092505.
[21] K. Matsubayashi, T. Terai, J.S. Zhou, Y. Uwatoko, Superconductivity in the topological insulator Bi2Te3 under hydrostatic pressure, Physical Review B, 90 (2014) 125126.
[22] A. Nakayama, M. Einaga, Y. Tanabe, S. Nakano, F. Ishikawa, Y. Yamada, Structural phase transition in Bi2Te3 under high pressure, High Pressure Research, 29 (2009) 245-249.
[23] G. Parthasarathy, W.B. Holzapfel, High-pressure structural phase transitions in tellurium, Physical Review B, 37 (1988) 8499-8501.
[24] F.P. Bundy, K.J. Dunn, Pressure dependence of superconducting transition temperature of high-pressure metallic Te, Physical Review Letters, 44 (1980) 1623-1626.

[25] Y. Akahama, M. Kobayashi, H. Kawamura, Structural phase transitions in selenium up to 150 GPa, Japanese Journal of Applied Physics, 32 (1993) 22.
[26] K. Kirshenbaum, P.S. Syers, A.P. Hope, N.P. Butch, J.R. Jeffries, S.T. Weir, J.J. Hamlin, M.B. Maple, Y.K. Vohra, J. Paglione, Pressure-induced unconventional superconducting phase in the topological insulator Bi2Se3., Physical Review Letters, 111 (2013) 087001.
[27] P.P. Kong, J.L. Zhang, S.J. Zhang, J. Zhu, Q.Q. Liu, R.C. Yu, Z. Fang, C.Q. Jin, W.G. Yang, X.H. Yu, J.L. Zhu, Y.S. Zhao, Superconductivity of the topological insulator Bi2Se3 at high pressure, Journal of Physics: Condensed Matter, 25 (2013) 362204.
[28] A.P. Hammersley, S.O. Svensson, M. Hanfland, A.N. Fitch, D. Hausermann, Two-dimensional detector software: From real detector to idealised image or two-theta scan, High Pressure Research, 14 (1996) 235-248.
[29] A. Dewaele, P. Loubeyre, M. Mezouar, Refinement of the equation of state of tantalum, Physical Review B, 69 (2004) 092106.
[30] S.T. Weir, J. Akella, C. Aracne-Ruddle, Y.K. Vohra, S.A. Catledge, Epitaxial diamond encapsulation of metal microprobes for high pressure experiments, Applied Physics Letters, 77 (2000) 3400-3402.
[31] D. Jackson, J. Jeffries, W. Qiu, J. Griffith, S. McCall, C. Aracne, M. Fluss, M. Maple, S. Weir, Y. Vohra, Structure-dependent ferromagnetism in Au4V studied under high pressure., Physical Review B, 74 (2006) 174401.
[32] G.J. Piermarini, S. Block, J.D. Barnett, R.A. Forman, Calibration of pressure-dependence of R1 ruby fluorescence line to 195 kbar., J. Appl. Phys., 46 (1975) 2774-2780.
[33] W.L. Vos, J.A. Schouten, On the temperature correction to the ruby pressure scale, Journal of Applied Physics, 69 (1991) 6744-6746.
[34] P. Vinet, J. Ferrante, J.R. Smith, J.H. Rose, A universal equation of state for solids, Journal of Physics C: Solid State Physics, 19 (1986) L467.
[35] P. Vinet, J. Ferrante, J.H. Rose, J.R. Smith, COMPRESSIBILITY OF SOLIDS, Journal of Geophysical Research-Solid Earth and Planets, 92 (1987) 9319-9325.
[36] L. Zhu, H. Wang, Y. Wang, J. Lv, Y. Ma, Q. Cui, Y. Ma, G. Zou, Substitutional Alloy of Bi and Te at High Pressure, Physical Review Letters, 106 (2011) 145501.
[37] J.G. Zhao, H.Z. Liu, L. Ehm, Z.Q. Chen, S. Sinogeikin, Y.S. Zhao, G.D. Gu, Pressure-Induced Disordered Substitution Alloy in Sb2Te3, Inorganic Chemistry, 50 (2011) 11291-11293.
[38] M. Einaga, A. Ohmura, A. Nakayama, F. Ishikawa, Y. Yamada, S. Nakano, Pressure-induced phase transition of Bi2Te3 to a bcc structure, Physical Review B, 83 (2011) 092102.
[39] S. Klotz, J.C. Chervin, P. Munsch, G.L. Marchand, Hydrostatic limits of 11 pressure transmitting media, Journal of Physics D: Applied Physics, 42 (2009) 075413.
[40] W.L. McMillan, Transition temperature of strong-coupled superconductors, Physical Review, 167 (1968) 331-344.
[41] J. Bardeen, L.N. Cooper, J.R. Schrieffer, Theory of superconductivity, Physical Review, 108 (1957) 1175-1204.
[42] R.C. Dynes, McMillan's equation and the Tc of superconductors, Solid State Communications, 10 (1972) 615-618.

[43] J.J. Hopfield, On the systematics of high Tc in transition metal materials, Physica, 55 (1971) 41-49.
[44] J.S. Schilling, S. Klotz, Physical Properties of High Temperature Superconductors, in: D.M. Ginsberg (Ed.) Physical Properties of High Temperature Superconductors III, World Scientific, Singapore, 1992, pp. 59.
[45] A. Eiling, J.S. Schilling, Pressure and temperature dependence of electrical resistivity of Pb and Sn from 1-300K and 0-10 GPa-use as continuous resistive pressure monitor accurate over wide temperature range; superconductivity under pressure in Pb, Sn and In, Journal of Physics F: Metal Physics, 11 (1981) 623.
[46] Y.S. Hor, A.J. Williams, J.G. Checkelsky, P. Roushan, J. Seo, Q. Xu, H.W. Zandbergen, A. Yazdani, N.P. Ong, R.J. Cava, Superconductivity in CuxBi2Se3 and its implications for pairing in the undoped topological insulator, Physical Review Letters, 104 (2010) 057001.
[47] N.P. Butch, P. Syers, K. Kirshenbaum, A.P. Hope, J. Paglione, Superconductivity in the topological semimetal YPtBi, Physical Review B, 84 (2011) 220504.
[48] T.V. Bay, T. Naka, Y.K. Huang, A. de Visser, Superconductivity in noncentrosymmetric YPtBi under pressure, Physical Review B, 86 (2012) 064515.
[49] Y. Pan, A.M. Nikitin, T.V. Bay, Y.K. Huang, C. Paulsen, B.H. Yan, A.d. Visser, Superconductivity and magnetic order in the noncentrosymmetric half-Heusler compound ErPdBi, Europhysics Letters, 104 (2013) 27001.
[50] N.R. Werthamer, E. Helfand, P.C. Hohenberg, Temperature and Purity Dependence of the Superconducting Critical Field, Hc2. III. Electron Spin and Spin-Orbit Effects, Physical Review, 147 (1966) 295-302.
[51] K. Maki, Effect of Pauli paramagnetism on magnetic properties of high-field superconductors, Physical Review, 148 (1966) 362-369.
[52] Y. Lu, T. Takayama, A.F. Bangura, Y. Katsura, D. Hashizume, H. Takagi, Superconductivity at 6 K and the Violation of Pauli Limit in Ta2PdxS5, Journal of the Physical Society of Japan, 83 (2014) 023702.
[53] T. Klimczuk, K. Baroudi, J.W. Krizan, A.L. Kozub, R.J. Cava, Superconductivity in the niobium-rich compound Nb5Se4, Journal of Alloys and Compounds, 649 (2015) 906-909.
[54] S.V. Eremeev, G. Landolt, T.V. Menshchikova, B. Slomski, Y.M. Koroteev, Z.S. Aliev, M.B. Babanly, J. Henk, A. Ernst, L. Patthey, A. Eich, A.A. Khajetoorians, J. Hagemeister, O. Pietzsch, J. Wiebe, R. Wiesendanger, P.M. Echenique, S.S. Tsirkin, I.R. Amiraslanov, J.H. Dil, E.V. Chulkov, Atom-specific spin mapping and buried topological states in a homologous series of topological insulators, Nature Communications, 3 (2012) 635.
[55] K. Govaerts, M.H.F. Sluiter, B. Partoens, D. Lamoen, Homologous series of layered structures in binary and ternary Bi-Sb-Te-Se systems: Ab initio study, Physical Review B, 89 (2014) 054106.
[56] T. Valla, H. Ji, L.M. Schoop, A.P. Weber, Z.H. Pan, J.T. Sadowski, E. Vescovo, A.V. Fedorov, A.N. Caruso, Q.D. Gibson, L. Müchler, C. Felser, R.J. Cava, Topological semimetal in a Bi-Bi2Se3 infinitely adaptive superlattice phase, Physical Review B, 86 (2012) 241101.